Extended Abstracts of the 1996 International Conference on Solid State Devices and Materials, Yokohama, 1996, pp. 121-123

Invited

Ultra-Shallow Doping for Si Sub-0.1 μm Devices

S. Matsumoto
Department of Electrical Engineering, Keio University
Hiyoshi, Yokohama 223, Japan

Abstract

Ultra-shallow doping with depths less than 30nm will be required for sub-0.1μm CMOS devices. As alternative technologies for ultra-shallow junctions, two step excimer laser doping has been reviewed. Furthermore new doping method using surface reconstructed superstructure is presented. This method enables to control of the number of dopant atoms accurately.

1 INTRODUCTION

VLSI technologies toward smaller dimensions in device structure demand ever decreasing junction depths. The formation of ultra-shallow junctions is one of the key technologies in the development of the next generation VLSI. For achieving ultra-shallow junctions, standard ion implantation technology is confronting with the difficulty such as the inherent channeling effect, anomalous diffusion due to the damage, lateral diffusion under the mask and so on. In order to meet the requirement, various kinds of alternative technologies have been proposed. These are low-energy implantation with preamorphization, ultra-high vacuum low temperature epitaxy, gas-phase and solid state diffusion, and excimer laser doping. In the present paper, we address the alternative technologies for shallow junctions that have been developed in our laboratory. First, excimer laser doping have been reviewed. Then new doping method using surface reconstructed superstructure will be presented.

2 EXCIMER LASER DOPING

A new doping technique using ultraviolet(UV) excimer lasers has been developed to form ultra-shallow junctions of dopants in silicon [1]. Silicon substrates are immersed with doping gases such as B_2H_6 and AsH_3 in the chamber during laser irradiation. The incident laser fluences cause the melting of silicon and simultaneously create dopant atoms by photolysis or pyrolysis of doping gas molecules. Then dopant atoms are incorporated into a molten region by the liquid-phase diffusion. UV excimer laser beam is absorbed extremely near the silicon surface because of a large absorption coefficient of silicon at UV regions, resulting in ultra-shallow junctions.

As a variation of laser doping, we developed the two-step doping using excimer laser [2] [3]. It consists of the deposition of dopant films by laser CVD and the liquid phase diffusion of dopant atoms by laser melt.

An ArF excimer laser (λ = 193nm) with a full width at half-maximum (FWHM) of 17 ns and a repetition frequency of 2Hz was used for both processes. The samples were (100) CZ n type Si wafers with a resistivity of 7.5–12.5 Ω·cm. 5% B_2H_6 diluted with He was used for the deposition of boron Films.

The deposition of boron films as dopant sources was carried out by the ArF excimer laser irradiation on a silicon substrate perpendicularly in B_2H_6 ambient. The energy density of the laser beam (Ed_1) was varied from 33 to 80 mJ/cm^2, which was sufficiently small as compared with that of the melting of Si. The number of irradiated laser pulses (n_1) was varied from 1 to 200. The partial pressure of B_2H_6 was set at 0.5 Torr.

After the stage 1 process, B_2H_6 gas was evacuated from the chamber to avoid additional supply of adsorbed layers during laser irradiation. This procedure is important for controlling the quantity of dopants. Then the laser beam with the energy density sufficient high for the melting of silicon was irradiated on samples. The laser energy density (Ed_2) was kept at 0.7 J/cm^2 and the number of pulses (n_2) was varied from 1 to 100. The suffix of each parameter indicates stage 1 or 2. In this two-step doping, both the deposition and the incorporation processes are carried out in the same chamber successively.

Fig. 1 shows the dependence of sheet resistance on the pulse number of the step 2 process (1, 10, 50, and 200). For comparison, the data of sheet resistance, which were obtained with the excimer laser doping in B_2H_6 ambients (0.5 torr) in a ordinary way, are also shown with a dashed curve. In this ordinary process, the sheet resistance varies sharply with the pulse number and then it is difficult to control the sheet resistance. On the other hand, the sheet resistance is almost independent of the pulse number of the step 2 process in the present two-step doping. Thus, the sheet resistance can be determined mainly with the pulse number of the step 1 process. The other advantage of this method is that a very low sheet resistance can be obtained even by only the one pulse irradiation for the melting of silicon.

The other advantage of this method is that the doping is performed in a simple condition. Figure 2 show the boron concentration profiles with 1 pulse of Si melting. Profiles are expressed by Gaussian distribution with very shallow junctions and controlled surface concentrations.

We applied this method to the fabrication of MOSFET on SOS [4]. Samples were processed at room temperature except the deposition of gate oxide at 450°C by LPCVD. Thus, this method can be applicable to amorphous on poly crystalline silicon on the glass. Figure 3 show the basic SOS TFT structure and key fabrication sequence. High-quality thin film transistors were fabricate with on/off current ratio of 7 and a field effect hole

mobility of 145 $cm^2/V{\cdot}S$

3 DOPING FROM ORDERED BORON SURFACE SUPERSTRUCTURE

Delta-doping or atomic layer doping has been studied for the formation of ultra-shallow junctions, punch through stopper in MOS devices [5] [6]. Confinement of dopant atoms has been performed by deposition of dopant source in MBE where dopant atoms are generally retained within a few monolayers of an interface. They are distributed at the substitutional sites randomly.

Recently, the reconstruction of Si(111) surface with boron adsorption is of much interest from possibility for new metastable materials and two dimensional structures. Boron is known to cause the surface to favor a $\sqrt{3}\times\sqrt{3}$R30° reconstruction over the Si(111)7×7 surface and to occupy a subsurface substitutional site directly below a Si adatom at a T_4 position [7–9].

We explore the possibility of using this ordered $\sqrt{3}\times\sqrt{3}$B superstructure as a diffusion source to form ultra-shallow junctions [10]. Significant advantage of doping from boron superstructure over the previous delta-doping is that the number of surface dopant atoms is kept to be constant since $\sqrt{3}\times\sqrt{3}$ superstructure form the ordered structure with coverage of 1/3 monolayers of boron. This point is particularly important in very small devices.

The formation of $\sqrt{3}\times\sqrt{3}$ reconstructed structures was performed in a gas-source Si-MBE apparatus (Bentec). Single crystalline n-type (111) CZ-Si wafers with resistivity of 8–15Ω·cm were precleaned by chemical treatment and a protective thin oxide film was formed. Then the oxide layer was sublimated at 830°C for 10min. A Si(111)-7×7 RHEED pattern was obtained after this surface cleaning process. The temperature of the substrates was lowered to 690°C and to obtain clean and smooth surfaces a buffer layer of about 50Å Si layers were grown using Si_2H_6. Boron was deposited from B_2H_6 gas at 690°C. Surface reconstruction from 7×7 to $\sqrt{3}\times\sqrt{3}$ was observed by RHEED. The undoped Si capping layers with a thickness of several nm were grown on the B layer.

The boron concentration was measured by SIMS (Atomika 6500) using O_2 primary ions. The sheet hole concentration and Hall mobilities were measured by the van der Pauw method.

Boron concentration profile in Si/B/Si(111) structures grown at 650°C is shown in Fig. 4. The full width at half maximum (FWHM) is 4nm. The boron profile by SIMS is, however, rather broad at low concentrations. Since B_2H_6 exposure was stopped just after the observation of the $\sqrt{3}\times\sqrt{3}$ pattern, the boron coverage is considered to be 1/3 layer. On the other hand, as SIMS measurement has its limitation in terms of the depth resolution, it might be responsible for the broad profile.

Fig. 5 shows the dependence of the sheet carrier concentration on the B_2H_6 exposure time. The growth temperature was 690°C and the B_2H_6 flow rate was 0.5 sccm. The sheet carrier concentration increased linearly with and increase of the B_2H_6 exposure time up to 100s and saturates above 100s. The saturation value of sheet carrier concentration is found to be almost 1/3 of the atomic density of Si(111) plain ($7.8\times10^{14}cm^{-2}$). As described by Hirayama et al, the $\sqrt{3}\times\sqrt{3}$B structure completes with a coverage of 1/3 monolayer. Therefore around 100s, the $\sqrt{3}\times\sqrt{3}$B structure is formed.

The sheet carrier concentration, N_s versus boron sheet concentration, N_B, is shown in Fig. 6. The sheet carrier concentration is varied from 10^{12} to $10^{14}cm^{-2}$ by changing the exposure time of B_2H_6 gas. The solid line shows a ratio $N_s/N_B = 0.70$, indicating that boron atoms were almost incorporated and electrically activated. At a large sheet concentration of boron, surplus boron atoms might exist on the non-active sites.

4 Conclusion

As alternative technologies for ultra-shallow junctions, two doping methods; excimer laser doping and doping using surface reconstructed superstructure, have been presented. Excimer laser doping consists of two-step process, deposition of dopant film and liquid phase diffusion of dopant atoms. This method will be applicable to TFT fabrication on the glass plates. New doping method using surface reconstructed superstructure has a significant advantage in controlling the number of dopant atomic accurately as well as the formation of ultra-shallow junctions.

References

[1] P. G. Carey, K. H. Weiner, and T. W. Sigmon, IEEE Electron Device Lett., 9 (1988) 542.

[2] S. Inui, T. Nii, and S. Matsumoto, IEEE Electron Device Lett., 12 (1991) 702.

[3] T. Akane, T. Nii, and S. Matsumoto, Jpn. J. Appl. Phys., 31 (1992) 4437.

[4] T. Nii, S. Matsumoto, and T. Matsuda, IEEE Electron Device Lett., 15 (1994) 72.

[5] C. E. C. Wood, G. Metze, J. Berry, and L. F. Eastman, J. Appl.Phys., 51 (1980) 383.

[6] D. A. Grützmacher, K. Eberl, A. R. Pwell, B. A. Ek, T. O. Sedgwick and S. S. Iyer, Thin Solid Films, 225 (1993) 163.

[7] H. Hirayama, S. Baba and A. Kinbara, Japan. J. Appl. Phys. 25, L452 (1986)

[8] V. V. Korobtsov, V. G. Lifshits and A. V. Zotov, Surf. Sci. 195, 466 (1988)

[9] R. L. Headrick, I. K. Robinson, E. Vlieg and L. C. Feldman, Phys. Rev. Lett. 63, 1253 (1989)

[10] H. Uji, S. Tatsukawa and S. Matsumoto, J. of Crystal Growth, 157 (1995) 105

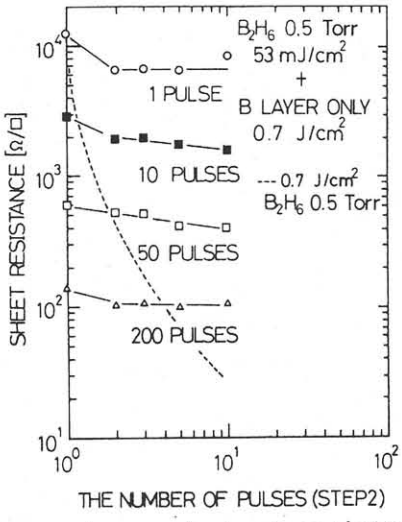

Fig. 1 Dependence of sheet resistance on the pulse number of the step 2.

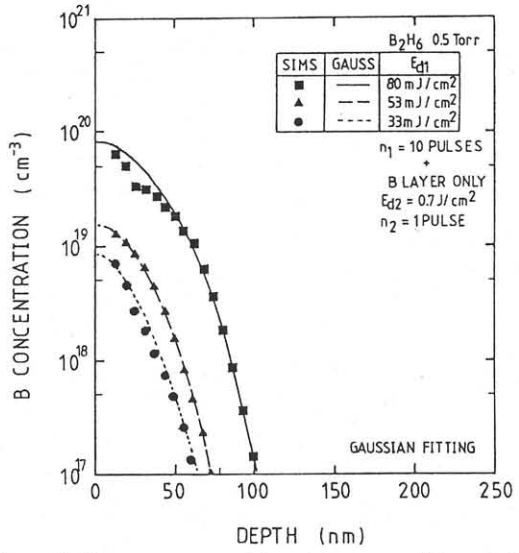

Fig. 2 Boron concentration profiles for different energy density of the depositing pulse.

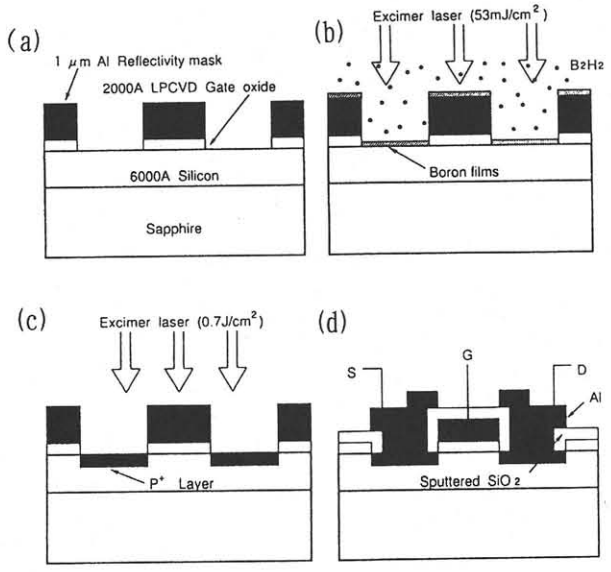

Fig. 3 Basic SOS MOSFET structure; (a) gate patterning, (b) boron film deposition by LCVD, (c) source/drain formation by laser melting, and (d) final structure.

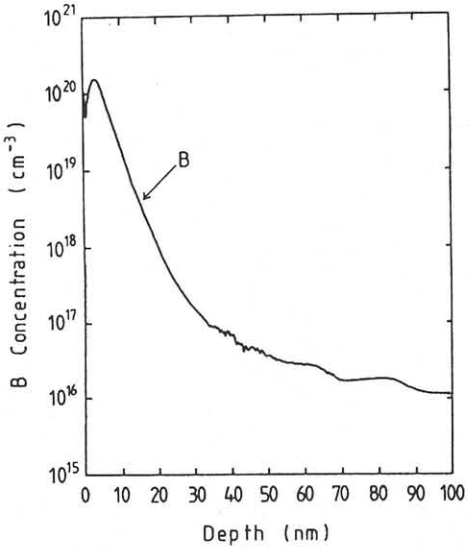

Fig. 4 SIMS boron profile of Si/B/Si(111).

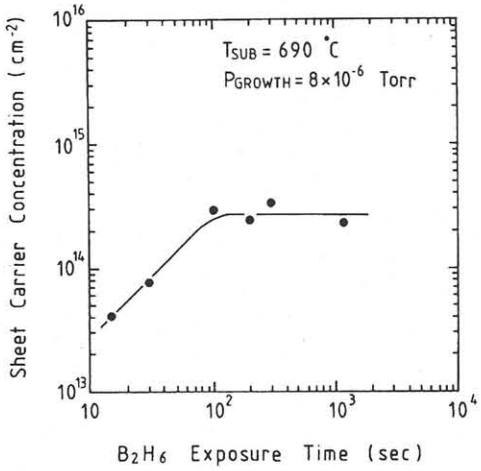

Fig. 5 Dependence of sheet carrier concentration on B_2H_6 exposure time.

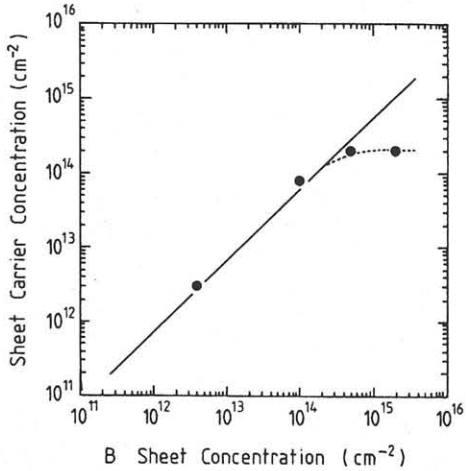

Fig. 6 Dependence of sheet carrier concentration on boron sheet concentration